

# Magnetic field visualisation and inductance calculation of a simple configuration surface coil at low magnetic field

A.O. Rodríguez\* and R. Amador\*\*

*Centro de Investigación en Imagenología e Instrumentación Médica, Universidad Autónoma Metropolitana Iztapalapa, Av. San Rafael Atlixco 186, México, D.F., 09340. México.*

R. Rojas

*Louisiana State University, Health Science Center, School of Medicine, Department of Radiology, 1542 Tulane Ave., Room 308, New Orleans, LA 70112, USA.*

F.A. Barrios

*Instituto de Neurobiología, UNAM-Juriquilla, Juriquilla 76230, Querétaro, México.*

Recibido el 28 de enero de 2004; aceptado el 30 de marzo de 2005

We propose a simple method based on the quasi-static approach to visualise the magnetic field created by a simple configuration coil using the calculation for coil inductance. Faraday's law was used to calculate the inductance value and to simulate the magnetic field produced by circular-shaped and square-shaped coils. A software tool was developed to compute the coil inductance, and display the simulated magnetic field. We compared the predicted measured values of inductance, and performed a comparison plot of area versus inductance for both coils. Three dimensional plots of simulated fields are also shown. A circular-shaped coil was built using the method reported here, and brain images were acquired. This approach proved to be useful as an aid to visualise the magnetic field generated by simple coil geometries, and, simultaneously, calculate their coil inductance values.

*Keywords:* Inductance; RF coil; simulation; magnetic field visualisation; magnetic resonance imaging; brain.

Un método simple basado en el enfoque cuasiestático se propone para visualizar el campo magnético creado por una antena, a través del cálculo de la inductancia de la antena. La ley de Faraday se emplea para calcular el valor de la inductancia y simular el campo producido por una antena circular y una antena cuadrada. Una herramienta software se desarrolló para obtener la inductancia de la antena y visualizar su campo magnético. Comparamos los valores experimentales y teóricos de la inductancia, graficamos el área de la antena versus la inductancia para ambos geometrías. Se obtuvieron gráficas tridimensionales para mostrar la simulación del campo magnético. Construimos una antena circular basada en este método para generar imágenes cerebrales. Este método muestra que es posible calcular la inductancia y visualizar el campo magnético de antenas RF con geometrías simples.

*Descriptores:* Inductancia; antena RF; simulación; visualización campo magnético; imagenología por resonancia magnética; cerebro.

PACS: 42.30.Va; 76.60.Lz; 76.60.Pc; 87.57.-s; 87.61.-c; 87.61.Cd; 87.63.-d

## 1. Introduction

Radio frequency surface coils have become a widespread commodity in both Magnetic Resonance (MR) imaging and MR spectroscopy since their introduction in the early 1980's [1]. A detailed description of the principles of magnetic resonance imaging can be found in Ref. 2. Understandably so; these devices are simple, inexpensive and very versatile, and can be used in many different shapes such as rectangular, square, elliptical, circular and so forth. The popularity of surface receiving coils is due to their superior spatial selectivity and signal-to-noise ratio (*SNR*), compared to those coils able to surround the entire sample. Because of its simplicity of construction, the circular loop coil has received the widest attention and it is commonly used in a number of applications ranging from imaging the heart, brain, and joints, for example. This particular type of coil, which can produce a higher *SNR* for a limited region, is usually made of copper substrate and a network that is necessary to maximise power transfer from the loop to the RF amplifier. This kind of array can be modelled as a coaxial transmission line.

A great deal of effort has been expended developing Magnetic Resonance Imaging and Spectroscopy (MRIS) coils, and much of the design technique is heuristic. Although the physical principles are established and software has been developed to help researchers design RF coils, these tools are mainly used for bird-cage coil. Not much attention has been given to developing the aids for the study of surface coils for MRIS. The International Society for Magnetic Resonance in Medicine has contributed to this end with some educational material mainly focused on providing practical guidelines to build both surface and volume coils [3]. Scientists and students interested in starting to study the behaviour of surface coils can be help by the graphical tools to understand some of the characteristics governing the performance of MR surface coils.

It is well known that the coil inductance for various configurations can be easily obtained, but these expressions cannot offer information on the form of the magnetic field generated by the coil. In this paper, a method based on the quasi-static approach is introduced to estimate both the inductance and the magnetic field isolines associated with the most pop-

ular surface coils shapes: circular and square-shaped coils. The geometry of the magnetic field produced by a surface coil is clearly an important factor in the behaviour of the inductance and the coil performance. A software tool based on computation of the magnetic field generated by a surface coil and its inductance is proposed in this article. This software programme is intended to help scholars and researchers understand important characteristics of a surface coil. The computational tool developed is able to generate 3D plots of the magnetic field as well as to compute the inductance of two types of receive coil: circular and square-shaped coils. Bringing these two aspects together in one tool allows us to study the two important aspects of single-loop coils behaviour. This can be of particular interest to anyone starting to develop this kind of RF coil or trying to engage in more complicated arrays, such as array coils [4], SENSE coils [5], SMASH coils [6], and PERES coils [7].

The article is structured as follows: a brief review of the characteristics and functions of a conventional surface coil is presented. Special attention is given to coil inductance since it also calculation of the magnetic field generated by the coil possible. Mathematical expressions for calculating the inductance are derived from the classical theory of electromagnetism for the circular-shaped and square-shaped coils. A software aid is then developed that simultaneously obtains the inductance, and it is able to generate a bi-dimensional plot of the magnetic field of an RF coil with an arbitrary size for the geometries mentioned above. To test the validity of this approach, experimental inductance values were obtained and compared to those predicted with the theory. Finally, a circular coil was built with the aid of this software tool and was tested on a clinical MR imager. Brain images of a healthy volunteer are shown. This research concludes with the technical remarks concerning the validity of this approach in the study of the properties of receive surface coils and describes some prototypes that were built using this technique.

## 2. Radiofrequency coils for magnetic resonance imaging

Radio frequency (RF) coils have two important functions in an MR system, transmission and reception of the MR signal, however, there are also coils that can operate in both modes, the so-called transceiver coil. In the transmission case, the RF coil serves as a transducer which converts RF power into a transverse rotating RF magnetic field in the imaging volume. High efficiency for this transmit mode of operation corresponds to the maximum magnetic field in the sample volume for minimum RF power. For the reception mode, the RF coil and its associated preamplifier serve as a transducer which converts a precessing nuclear magnetisation into an electrical signal suitable for further signal processing. High efficiency for this reception mode corresponds to a minimal degradation of the inherent signal-to-noise ratio (*SNR*) of the sample volume. In this case, coils are the component of the MR imager directly in contact with the object to be imaged.

A well-designed coil can be highly efficient as both a transmitter and a receiver. For MRI it is also desirable for the excitation and reception to be spatially uniform in the imaging volume. Unfortunately spatial uniformity and high-efficiency can not both be optimised simultaneously. Increasing the spatial uniformity will augment the required power and decrease the *SNR*. In contrast an RF transmit coil needs to store magnetic energy temporarily with minimal dissipation and preferably no radiation. Although the sample material may absorb significant RF energy, only a minuscule fraction of it is actually absorbed by the nuclear spins. Similarly, the RF receive coil detects the rotating nuclear magnetisation without extracting any significant energy from the nuclear spins. Such transfer of energy from the spins to the RF coil will cause a shortening of the free induction decay. Viewing the RF coil as a magnetic storage device is a key to good choice design. Efficiency energy storage optimises both the transmit and receive performances of a coil assembly. Resonant circuits are a natural choice for magnetic energy storage.

Many different coils have been developed and, according to their shape can be categorised into main groups. The first group is called volume coils, which include Helmholtz coils, saddle coils, and high-pass and low-pass birdcage coils. The second group is called the surface coil, which includes single-loop and multiple-loop coils of various shapes. These coils are usually much smaller than the volume coils and, hence, have a higher *SNR* because they receive noises only from nearby regions. However, they have a relatively poor magnetic field uniformity and these are mainly used as receive coils. Fig. 1 shows some schematics and photos of RF coils commonly used for MRI.

RF coils are relatively complicated structures. It is difficult and time consuming to analyse them exactly based on the Maxwell's equations. However, for RF coils whose size is a small fraction of a wavelength, we can use the so-called equivalent circuit method to analyse them. The basic principle of this method is, first to establish an equivalent lumped-circuit for the coil by modeling a conducting wire or strip as an inductor, then to analyse the equivalent circuit using the well-known Kirchhoff's laws and, finally, to calculate the magnetic field using Biot-Savart's law. This method is highly efficient, reasonably accurate, and thus very practical for the design of RF coils. Some equivalent circuits of RF coils are shown in Fig. 2.

### 2.1. Radiofrequency subsystem of an mr imager

The function of this part of the apparatus is to apply RF magnetic field pulses to the appropriate region of interest, and to receive the weak MR signal emanating from the region of interest. The RF electronics of an MR system are designed to generate the pulsed RF output required to excite magnetic resonance and to prepare the signals picked up by the coil for the image processor. The signal paths are illustrated in Fig. 3.

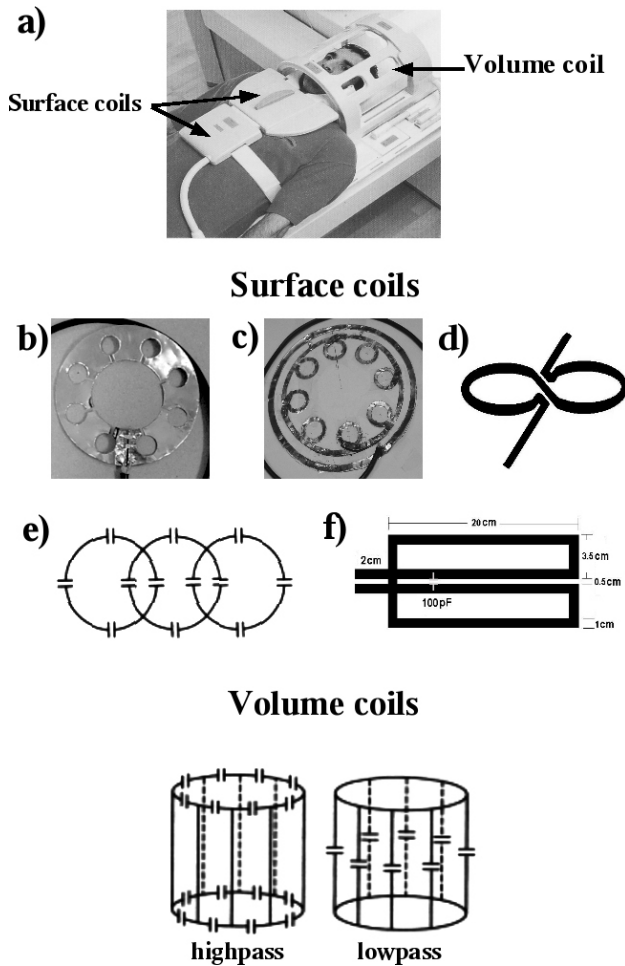


FIGURE 1. Schematics and photos of some RF coils used in various magnetic resonance imaging applications. a) both surface and volume coils showing their use in practice. Surface coils: b) Planar magnetron coil with 8 cavities [8], c) PERES coil with circular envelope [9], d) Folded Crossed-Ellipse Coil[10], e) phased-array coils [4], Ampere coils for hand and arm imaging [11]. Volume coils: popular birdcage coils.

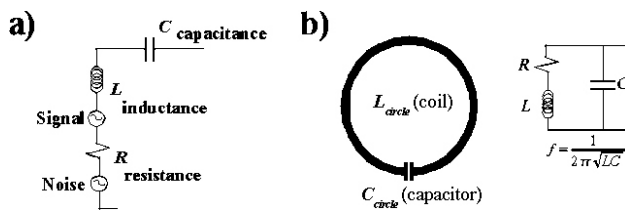


FIGURE 2. Equivalent circuits of conventional surface coils: a) generic equivalent circuit, and b) equivalent circuit of a circular-shaped coil. The inductive reactance  $j2\pi fL$  cancels the capacitive reactance  $(j2\pi fC)^{-1}$ , and hence the resonant frequency becomes Eq. (4).

RF coils are a very important part of the RF subsystem since they are responsible for receiving and transmitting the magnetic resonance signals.

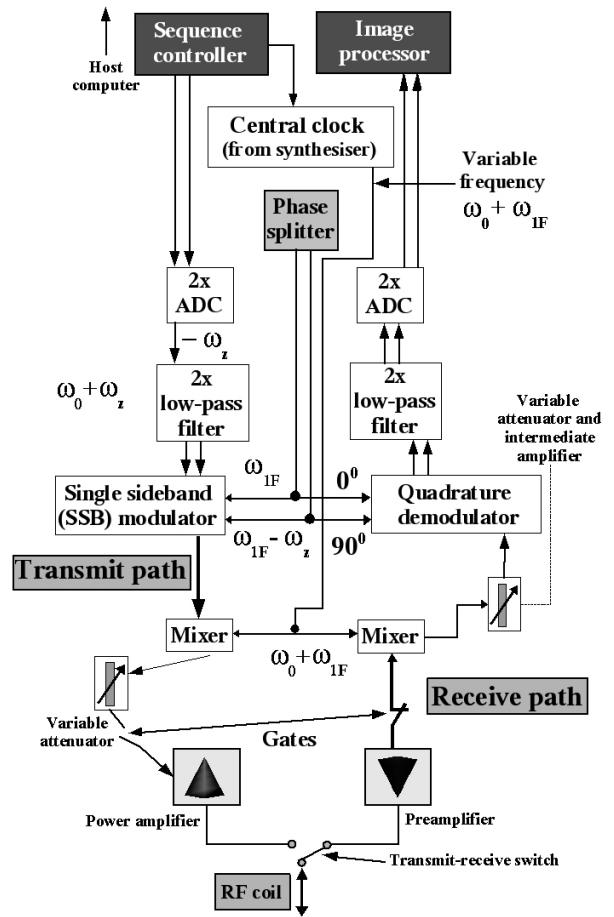


FIGURE 3. Diagram of the RF subsystem of a magnetic resonance imager. The received and transmitted paths are illustrated.

### 2.2. RF coils and the signal-to-noise ratio

While coils are, to a degree, frequency discriminating, they do not discriminate between currents induced by the transverse magnetisation representing tissue MR behaviour (signal), and the portion of black-body radiation generated by the motion of molecules (thermal noise) that happens to be aligned in the transverse plane at the MR frequency. This noise degrades image quality in all situations. The slice selective [2] approach to MRI causes signal to be generated only by part of the tissue in the sensitive volume of the coil but noise comes from all of the coil volume. Therefore, it is best to select a coil with a sensitive volume that matches the target volume (useful field of view in 3 dimensions) as closely as possible. As long as the target volume is included in the coil sensitive volume, the smaller the coil the higher the SNR. Typical MRI imagers are available with body, head, and extremity coils and a range of anatomy specific surface coils, although the range and quality of coils varies between manufacturers and MR systems (see Fig. 1). The MR radiographers must choose the most appropriate coils for examination to ensure optimum results. In day-to-day operation, the selection of an appropriately sized coil is the primary means

of assuring the best image quality. A widely accepted form to measure the performance of an RF coil is the *SNR*.

An MRI experiment involves the combination of two important parameters, signal and noise. This can be referred as the *SNR*. This parameter is an accepted standard for measurement of quality in MRI studies. The MR signal is determined by the magnetic field generated by the coil. Noise always accompanies a signal that is not solely due to the coil itself, but the human body too. The biological sample (patient) produces a resistance that is comparatively large, since it is a poor conductor, and contributes significantly in the noise figure induced to the coil. To include the biological sample resistance, the *SNR* expression is [12-13]:

$$SNR = \frac{\text{Peak signal}}{\text{RMS noise}} \quad (1)$$

$$SNR_{\text{square}} = \frac{MV\sqrt{l}}{\sqrt{\left(\frac{l^2}{2} + z_p^2\right)\left(\frac{l^2}{4} + z_p^2\right)}\sqrt{16\pi kT\Delta f\sigma\left(\frac{1-\sqrt{2}}{3} + \ln(1+\sqrt{2})\right)}} \quad (3)$$

where  $l$  is the length of one side of the square-shaped coil. Eqs. (2) and (3) are based on the model of a lossy half-space in the quasi static case. The coils are assumed to have no conductive loss and the noise is dominated by the sample. It is worth mentioning that the model of a conductive half-space used here is adequate for cases in which the coils are small compared to the sample. Equivalent expressions can be found for volume coils like the traditional birdcage coil.

### 2.3. Equivalent circuit of a conventional surface coil

Surface coils are generally operated as resonant circuits. Therefore an equivalent circuit can be formulated to study the parameters affecting the design of an RF coil [15]. In a resonant circuit, equal amounts of energy are stored in the electric and magnetic fields, with the energy exchanging repeatedly between the electric and magnetic fields. Electric fields with lossy dielectrics (patients) lead to increased resistance in the coil, the electric fields should be associated with the capacitors used for tuning and matching the coil rather than the stray electric field of the coil. Surface coils can be regarded as a resonant circuit, being composed of a resistance  $R$ , and inductance  $L$ , and a capacitance  $C$ . These circuits are commonly called *RLC* circuits. The design of MRI surface coils strongly depends on these parameters. Consequently, using Kirchhoff's law for circuits in Fig. 2b, it can be obtained that the resonant frequency,  $f$  is:

$$f = \frac{1}{2\pi\sqrt{LC}} \quad (4)$$

The simulation of an equivalent circuit to calculate the key parameters of a MRI coil provides us with a way to save

In particular, the quasi-static *SNR* of a circular-shaped coil as a function of a given depth  $z_p$  is [14]:

$$SNR_{\text{circle}} = \frac{MV\sqrt{a}}{\sqrt{(a^2 + z_p^2)^3}\sqrt{16kT\Delta f\sigma}} \quad (2)$$

where  $M$  is the magnetisation density,  $V$  is the voxel,  $k$  is the Boltzmann constant,  $\Delta f$  is the receiver low-pass filter,  $T$  is the temperature of the loss resistance,  $\sigma$  is the conductivity of the half-space,  $a$  is the coil radius, and  $z_p$  is the depth of the observation point. Similarly, the squared-shaped coil *SNR* is [14],

a considerable amount of time and effort. Fig. 2 shows some equivalent circuits for RF coils.

### 2.4. Quality factor of an RF coil

To provide a quantitative way to measure the quality of the circuit, a quality factor,  $Q$  can be defined as the energy stored divided by the energy dissipated per period. The  $Q$  of a resonator can be expressed as [15]:

$$Q = \frac{fL}{R_{\text{coil}}} \quad (5)$$

From Eq. (5), it can be said that a high  $Q$  should have a small resistance. The higher the  $Q$ , the higher the ratio of flux density produced to power dissipated in the coil. Typical values for loaded coils range from the order of magnitude of 10 to that of 100. The relative values of  $R_{\text{coil}}$  and  $R_{\text{sample}}$  can be determined by measuring the  $Q$  when the coil is empty and when it is loaded by a patient or a phantom (water-filled bottle). The best indicator of the coil sensitivity is the ratio:

$$\frac{Q_{\text{empty}}}{Q_{\text{loaded}}} = \frac{R_{\text{coil}} + R_{\text{sample}}}{R_{\text{coil}}} \quad (6)$$

provided the dielectric losses do not contribute to  $R_{\text{sample}}$  (patient). This ratio can be 5 times or more for a magnetic field strength of 1.5 Tesla; thus coil losses contribute less than 11% of the observed noise value. Therefore, a good coil design should have a  $R_{\text{sample}} \gg R_{\text{coil}}$ . A much simpler approach is to calculate  $Q$  according to the following expression [16]:

$$Q = \frac{f}{\Delta f} \quad (7)$$

where  $\Delta f$  denotes the bandwidth, which can be measured easily with the aid of a network analyzer. The measured  $Q$  factor includes the contribution of the capacitor's resistance, and one must be aware that many capacitor manufacturers specify the  $Q$  of their products. High quality chip capacitors are thus recommended to be used in the design of an MRI coil, to avoid unwanted resistance contributions coming from these electronic components which can drastically affect the quality factor.

### 3. Inductance calculation of a surface coil

The resistance and inductance depend on the shape of the coil. Of particular interest is the inductance, because it allows us to study the energy stored in a coil and its relation to the magnetic field. The physical inductance can be studied using the magnetic flux model as in classical electromagnetism. It is well known that inductance  $L$  is defined as

$$L = \frac{1}{i} \int_s B \cdot dS, \quad (8)$$

where  $B$  is the magnetic field in the cross-section of area  $S$  and  $i$  is current. Eq. (8) shows that the magnetic field in this area  $S$  is proportional to the current and inductance. It can also be proved that, for a constant current, there is a direct relationship between the magnetic field of the surface coil and its inductance. This is an important aspect to be considered in developing surface coils for MR imaging and spectroscopy. This inductance formula (Eq. (8)) provides a way to actually map the pattern of the dependence of spatial coordinates on the magnetic field generated by the surface coil. The mea-

surement of inductance and capacitance of an RF coil is an important aspect when constructing coils dedicated to MRIS. In the case of simple geometries such as the circular and squared-shaped coils, several equations to estimate the inductance of the coils have been proposed. Bueno and coworkers [17] have shown that all these mathematical expressions of inductance are equivalent. In addition other methods have been introduced that are both analytical [18-19] and numerical [20] to compute the inductance of a surface coil. The inductance of circular and square coils was obtained using Eq. (8), where the corresponding magnetic field was first calculated using the Biot-Savart law.

A position-dependent function is required to map, point by point, the magnetic field generated by a surface coil. This approach can give a spatial resolution to the magnetic field for a particular shape of surface coil. Eq. (8) together with the calculation of the magnetic field of a circular-shaped coil (see Appendix), an inductance formula can be derived:

$$L_{cir} = \frac{R\mu_0}{2} \int_0^R \int_0^{2\pi} \frac{(R - x \cos(\omega))}{(R^2 + x^2 - 2Rx \cos(\omega))^{3/2}} d\omega dx \quad (9)$$

where  $R$  is the coil radius,  $x$  is the distance between the coil centre and an arbitrary point,  $\omega$  is the angle formed by the radius  $R$  and the distance  $x$ , and  $\mu_0$  is the permeability. Eq. (9) shows that coil inductance can be obtained via the calculation of the coil magnetic field, which is a function of the coil radius and position  $x$ .

The analytical expression to compute the inductance of a square-shaped coil can similarly be found as in Eq. (9). The inductance formula is:

$$L_{sqr} = \frac{\mu_0}{4\pi} \int_0^x \int_0^y \frac{\lambda}{x} \left[ \frac{l-y}{\sqrt{(l-y)^2 + x^2}} + \frac{y}{\sqrt{y^2 + x^2}} \right] + \frac{\lambda}{l-y} \left[ \frac{l-x}{\sqrt{(l-x)^2 + (l-y)^2}} + \frac{x}{\sqrt{(l-y)^2 + x^2}} \right] dx dy \\ + \frac{\mu_0}{4\pi} \int_0^x \int_0^y \frac{\lambda}{l-x} \left[ \frac{y}{\sqrt{(l-x)^2 + x^2}} + \frac{l-y}{\sqrt{(l-y)^2 + (l-x)^2}} \right] + \frac{\lambda}{y} \left[ \frac{x}{\sqrt{x^2 + y^2}} + \frac{l-x}{y^2 + (l-x)^2} \right] dx dy \quad (10)$$

where  $l$  is the square size. The magnetic field expression [Eq. (10)] on a square coil is dependent of the coil size (length of a side) and the position  $(x,y)$ . Unlike the majority of textbooks on electromagnetic theory (21-26), these inductance formulae above depend on the magnetic fields which are functions depending on the spatial coordinates  $(x,y)$  and the actual size of the coil. This approach provides a scheme to point-to-point map the magnetic field generated by the surface coil and calculate the inductance value for that particular configuration. It is necessary to find primitive functions for Eqs. (9) and (10). This can be a very complicated task, since no primitive functions exist to compute these integrals.

Hence, a possible solution can be found by using a numerical approach such as Simpson's rule.

### 4. Magnetic field simulation and inductance calculation

To compute the inductance of a surface coil with the formulae above [Eqs. (9) and (10)], it is necessary to first calculate the point-by-point magnetic field inside the RF coil. The magnetic field of the circular and square-shaped coils were

numerically computed. To obtain the point-by-point magnetic field within a circle as shown in Fig. 4a, the coil was centered at the origin of a coordinate system, and then concentric circles were then formed by increasing  $x$  until the entire area is covered (Fig. 4b,  $S$  was fully covered,  $x=R$ ). The magnetic field generated by the square-shaped coil was carried out by selecting a  $dx dy$  to form a differential of area inside the square depicted in Fig. 5a. This procedure was again repeated until the whole of the area was covered (Fig. 5b). In both cases, each different contribution represents the magnetic field at each point within the area formed by the coil geometry; therefore, the summation of all of them gives the total magnetic field inside the coil. Since the numerical solutions for the magnetic fields [Eqs. (A.7) and (A.20)] are highly-computationally demanding, all the numerical calculations of the magnetic field were done in Visual Basic (V.6, Microsoft Co., USA) with a 500 MHz Intel Pentium PC. A numerical simulation of the field can be easily displayed using these spatial data. To easily visualise the simulations of the magnetic fields, the data were imported into the spread

sheet MS Excel (Microsoft Office 2000) for plotting and files were created. A software tool was then developed to put together the output of the inductance calculation process and the visualisation of the magnetic field.

## 5. Software tool

To facilitate the study of the behaviour of the magnetic field and the inductance of these two surface coils, a software tool was developed. This programme can be used to calculate the inductance value of both circular and square-shaped coils which can be used as a guideline to build a coil prototype, and to illustrate the pattern generated by the magnetic field of the surface coil. Similarly, computer programme were specially written in Visual Basic to compute the integrals in Eq. (9) and (10) using Simpson's rule. The Excel application was also used to display the magnetic field in the form of three-dimensional plots. In Fig. 6, some plots produced by the programme are shown.

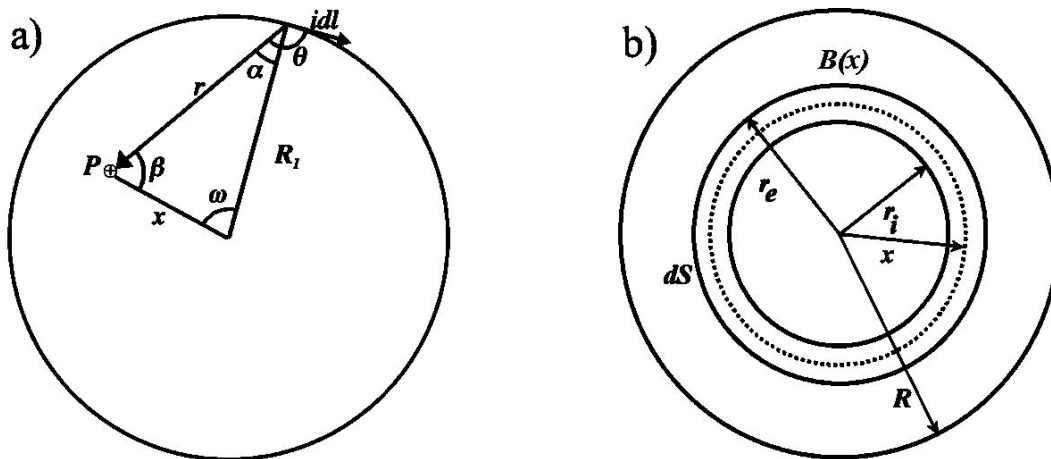


FIGURE 4. Calculation of the magnetic field of a circular coil. a) A vector diagram for an arbitrary point  $P$  which is selected inside the area of circle, then the distance ( $r$ ) from the point to a current element is measured. In order to obtain the contribution of this point, the distance to the centre ( $x$ ) and the circle radius ( $R$ ) are obtained too. The sine and cosine rules can be used to yield an expression to calculate  $r$ . b) Magnetic field  $B_{cir}(x, y)$  in a differential area of  $dx dy$  within the surface  $S$  (circle). All the contributions in the circle inside the area ( $S$ ) should be considered until the entire area is scanned.

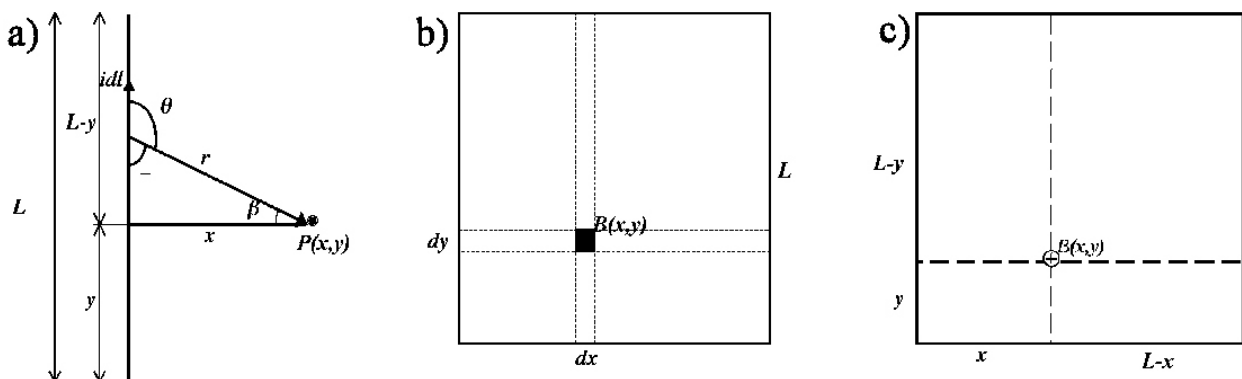


FIGURE 5. Calculation of the magnetic field of square-shaped coil. a) a side view of the square showing the vector diagram of the magnetic field applied on the point  $P$ . b) Schematic showing the integration limits for the four sides of the square-shaped coil. c) Magnetic field  $B_{sqr}(x, y)$  in a differential area of  $dx dy$  within the surface  $S$  (square).

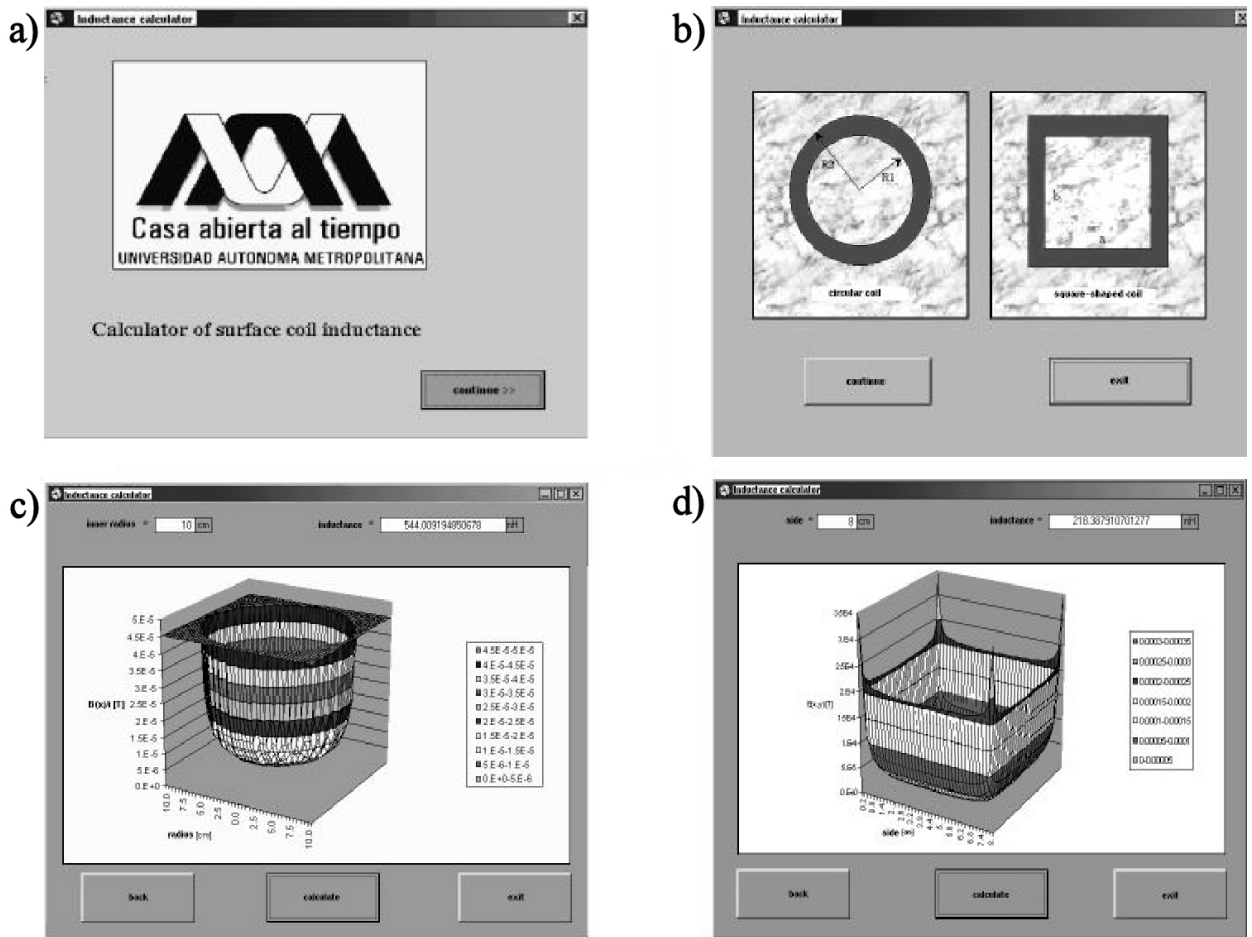


FIGURE 6. Some windows of the software tool to calculate the inductance of the surface coil are shown. a) starting page, b) coil selection page, c) mapping of magnetic field generated by a circular-shaped coil, and d) magnetic-field isolines of square-shaped coil.

### 6. Experimental inductance

In order to compare these theoretical results of both circular and square-shaped coils against experimental inductance values, coil prototypes of different sizes were built. Hence, resonant circuits were constructed by attaching a non-magnetic capacitor (American Technical Ceramics: series ATC 100B, non-magnetic) in series to each coil: the capacitor values were the same for all cases. A 50 Ω coaxial cable was also attached to the coil to conduct the signal. The inductance of a coil can be calculated by measuring its resonant frequency with a network analyzer (Advantest R3753 AH, Tokyo, Japan) provided the capacitor value is known. Since all measurements were done with a network analyzer, loss return plots were generated and the resonant frequency was measured for each coil. To finally obtain the coil inductance, the following formula was used:

$$L_{exp} = \frac{1}{4\pi^2 f^2 C} \tag{11}$$

where  $C$  is the capacitance and  $f$  the resonant frequency of the coil. Finally, to test the validity of this method, comparison plots of calculated and experimentally measured data for the two geometries were computed and shown in Fig. 7a

and 7b. The inductance plots show very good agreement between the inductance values obtained with the simulation and the experimentally-obtained inductance values. To compare the inductance of both coils, a plot of area versus inductance in each case was computed and shown in Fig. 8.

### 7. Development of a surface coil prototype

To use an RF coil for MRI applications, it is necessary to tune it to the specific resonant frequency and match it to 50Ω. The resonant frequency is determined by the species to be used, for example, 1H, 13C, 19F, 23N and 31P, which have a specific resonant frequency depending on the magnetic field strength [2]:

$$f = \frac{\gamma}{2\pi} B_0 \tag{12}$$

where the gyromagnetic ratio is  $\gamma$ ,  $B_0$  is the uniform magnetic field applied, and  $f$  is the Larmor frequency of the nucleus. In our case, we take the proton gyromagnetic ratio, 42.58 MHz/T. The 1H species is the most significant nucleus for most MRI studies because of this natural concentration in the human body as part of the water molecule and its high

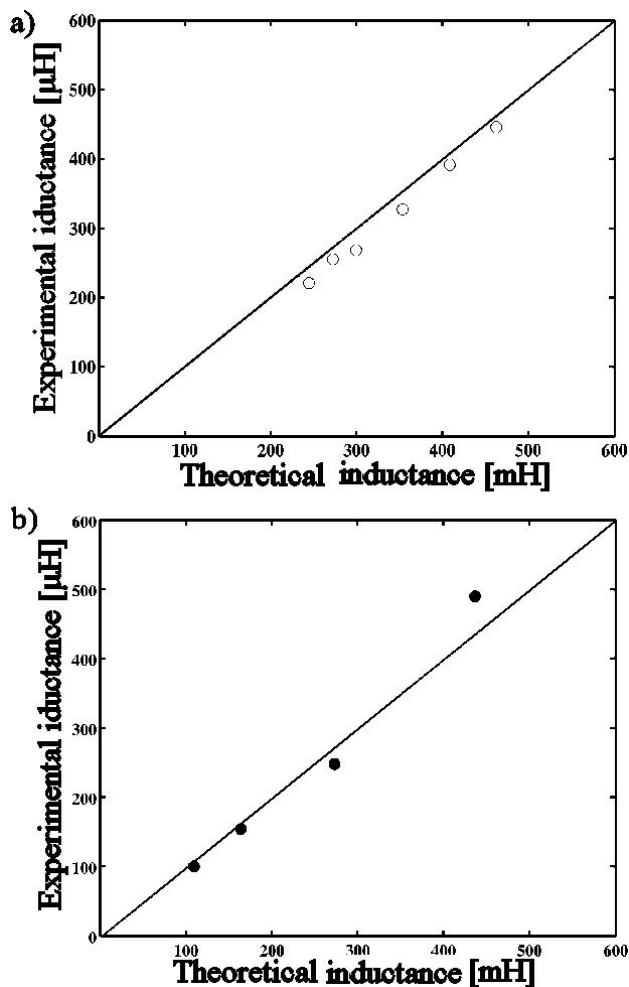


FIGURE 7. Comparison of the theoretical and experimental values of inductance (a) circular coil for radii: 4.5, 5, 6.5, 7.5 and 8.5 cm. (b) square-shaped coil for sides: 4, 6, 10, and 16 cm.

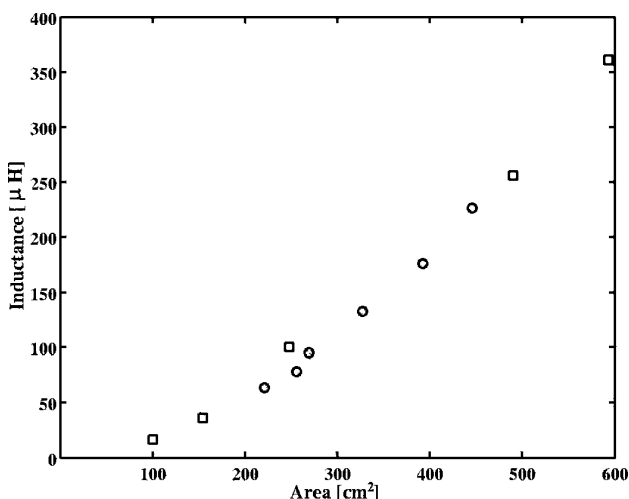


FIGURE 8. Comparison plot of inductance values of both coils as a function of the area. It can be appreciated that inductance for the tow coils is approximately the same.

NMR sensitivity. The high sensitivity of the  $^1\text{H}$  species can be intuitively understood by considering the fact that there is typically only one electron shielding the magnetic moment that the nucleus produces. This lack of shielding is even more pronounced for the hydrogen in water, where the nature of the O-H bond is covalent. This tends to remove the shielding electron from the  $^1\text{H}$ . The effect of this is to make the nucleus' state more easily permutable from external influences.

### 7.1. Resonant frequency tuning

A circular-shaped coil was then built with the aid of this software to resonate at 64 MHz. This is the resonant frequency of single protons when a 1.5 Tesla magnetic field is applied. Hence, the theoretical inductance of a 1 cm-wide strip coil with coil radius of 15 cm is 408 nH. From this result and Eq. (11), a chip capacitor (American Technical Ceramics: series ATC 100B non-magnetic) with a capacitance value 15.21 pF was attached in series to the coil to produce the desired resonant frequency. The circular-shaped coil was mounted and fixed on a rigid surface to facilitate tuning and matching of the coil prototype. Resonant frequency was measured with a network analyzer as indicated in Sec. 6. Fig. 9a shows the resonant frequency of the coil prototype.

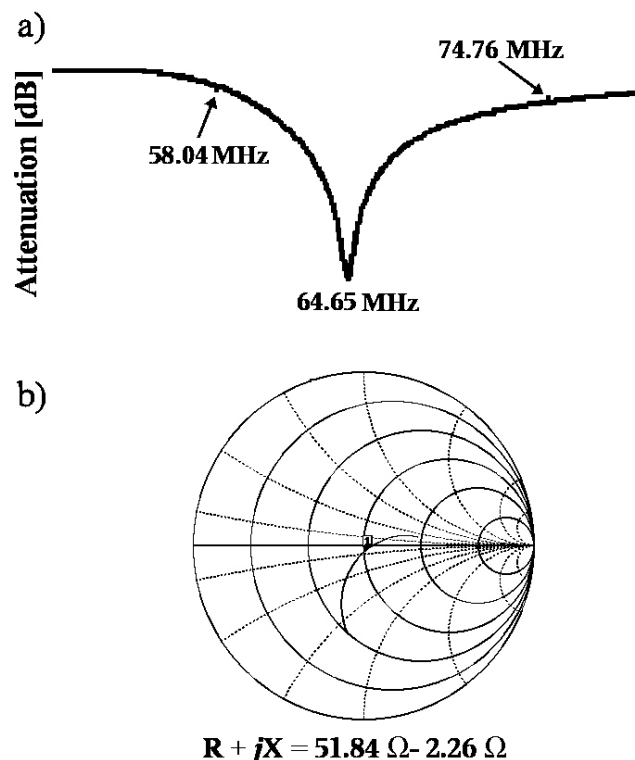


FIGURE 9. Coil characterisation: a) resonant frequency tuning and its bandwidth measured at 3 dB, and b) Smith chart showing 50  $\Omega$  matching. Quality factor of coil prototype was computed using Eq. (7), so  $Q = 31.4$ .

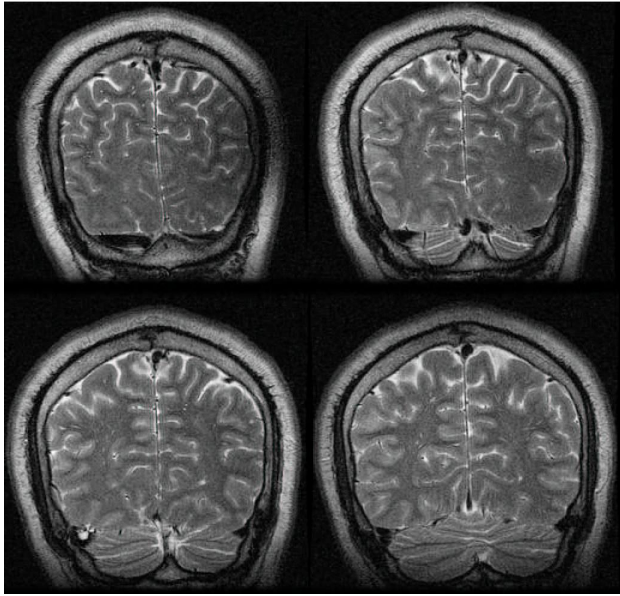


FIGURE 10. Coronal brain images obtained with a circular coil prototype designed with the aid of the software tool. Images were acquired with the following parameters: TE/TR = 171/3700 ms, FOV = 75 cm<sup>2</sup>, slice thickness = 4 mm, image size = 512 × 512.

## 7.2. 50 Ω matching

The frequencies employed in MRI are in the same range as those used for radio transmission, so to shield the signals coming from a region of interest, a coaxial cable is normally used. The type of cable imposes a constraint, the so-called characteristic impedance  $Z$  and only if, at the end of the cable, there is a termination of resistance  $R=Z_0$ . If  $R$  differs from the value  $Z_0$ , the power is reflected. Similarly, in general, if we measure the impedance between the conductors of a cable terminated with an impedance  $Z$  (*i.e.*  $Z$  is at the opposite end from our measurement), we will not record a value  $Z$ . Only if  $Z=R=Z_0$  will that value be recorded, the cable otherwise acts as an impedance transformer. Therefore, coils are usually matched to 50Ω to assure maximum energy transfer from the sample to the MR imager. The coil is connected to a network analyzer via a 50Ω coaxial cable to form a coaxial transmission line and to measure the resonant frequency and the 50Ω matching. Fig. 9b shows the resonant frequency of the coil prototype. The 50 Ω-coaxial transmission line (quarter wavelength) was also used to carry the MR signal to the preamplifier of the RF subsystem (see Fig. 3). The coil prototype was tested on a 1.5 Tesla Signa LX imager (General Electric Medical System, Milwaukee, WI, USA) together with standard clinical sequences, and brain images of a healthy volunteer were acquired. Fig. 10 shows brain coronal images obtained with a circular-shaped coil designed and built with this method.

## 8. Discussion

A simple approach was used to calculate the inductance of circular-shaped and squared-shaped coils for MRI. Analyti-

cal inductance expressions for both coils were derived and their solutions were found via numerical solutions. These solutions offered not only a way to compute their corresponding inductance values as a function of the coil size, but also a way to map the magnetic field generated by each coil configuration. Because of the highly computational nature of the solution, a software tool to automatically compute the inductance of both configurations was developed using widely available software.

Figure 6 shows the magnetic field associated to the corresponding coil configuration and the inductance value for a particular size ( $r$ , radius or  $l$ , square size). The encouraging results in Fig. 6 indicate that this software tool might be of some aid in obtain a preliminary value of the inductance of the coil, as well as in providing an idea as to how the prototype performs by plotting the magnetic field. The visualisation of the magnetic field can also facilitate the understanding of the uniformity patterns of the coils. These magnetic field plots are in very good agreement with those reported by Sobol in 1986 [26]. The magnetic field of a square-shaped coil generates high peaks of the magnetic field at the corners, see Fig. 6d. From Fig 6c & 6d, it can be seen that the magnetic field patterns of the circular coil and squared-coil show important differences. These contribute negatively to the image quality in the form of undesired artefacts. This can usually appear as image hyperintensities that mask out the relevant information. However, these defects can be easily diminished by chopping the corners off to get a more rounded shape.

Figure 7 shows that numerically-acquired inductance shows a very good agreement with the experimental inductance obtained with a network analyzer. It can be observed from Fig. 7 that calculation of coil inductance with the software tool developed here can serve as a guideline to calculate the coil size too. Coil size is an important issue in MRI, since coils having big radii tend to capture higher noise levels coming from bigger regions of interest; this effect degrades the image quality. It is then suggested small coils to be able to generate high SNR images. This approach is mainly used in phased-array coils, an example of this type of coil is shown in Fig. 1e. Knowing the inductance of a coil before building a coil prototype can save a considerable amount of time and effort. Figure 8 shows that the coil inductance for a similar area is approximately the same. This implies that both coil configurations can be used indistinctly. However, an advantage of the square coil over the circular coil is that the field uniformity of the former is slightly better than the latter one. Tuning, matching, and quality factor of coil prototype compare very well with those reported in the literature [27].

Since Microsoft products have been used to develop this software tool, a number of restrictions are applied by the company. Potential users must purchase the corresponding licenses to use Visual Basics and Excell programmes. The access to a wide number of potential users is drastically reduced due to license restrictions. Java language can be a good alternative in order to avoid these restrictions, because it can

be freely obtained and it is compatible with almost any computer platform available on the market. In addition, a number of potential users can gain access to this software tool on the Internet.

We have proved that a method to simultaneously calculate the inductance of a surface coil and simulate its magnetic field can be elaborated for simple coil configurations. The combination of these physical parameters can serve as a tool in designing coil with complex geometry. It is also possible to visualise the behaviour of the coil magnetic fields via the calculation of the coil inductance. These coils designed with this method did not require any further adjustments before operating on a clinical imager. This computational programme proved to be useful in building a coil prototype with a simple geometry for a commercial MR imager. It is also compatible with standard imaging sequences to generate quality brain images as shown in Fig. 10.

## 9. Conclusions

A software tool to compute the inductance of an RF coil as well as the visualisation of its magnetic field has been developed for simple RF coil configurations. The computational method proposed in this work offers an alternative approach to the trial-and-error method widely used in the development of RF coils for MRI. It has been proved that widely-available commercial software together with a first principle approach can be used to build a computational tool to assist researchers and scholars in the development of RF coils for MRI.

## Acknowledgements

We would like to thank Dr. Julián Sánchez-Cortazar, former Medical Director of American British Cowdray Medical Center-Mexico for the support needed to carry out this work. R. A. is grateful to National Council of Science and Technology of Mexico for a graduate scholarship.

## A Appendix: Calculation of surface-coil magnetic field

### A1. Circular coil

According to the Biot-Savart law in Fig. 1a, the magnetic field  $dB$  produced at  $P$  per current element time the change in magnetic field in length  $dl$  for a circular loop can be expressed as:

$$dB_{cir} = \frac{\mu_0}{4\pi} \frac{idl \sin(\theta)}{r^2} \quad (\text{A.1})$$

where  $r$  goes from current element,  $idl$  to the point  $P$ , and  $\theta$  is the angle between  $r$  current element directions. If we take  $R = R_1$  and apply the cosine rule, we obtain:

$$r^2 = R + r^2 - 2Rx \cos(\omega) \quad (\text{A.2})$$

$$x^2 = R + r^2 - 2Rx \cos(\omega) \quad (\text{A.3})$$

Also, if  $l = R\omega$  then  $dl = R d\omega$  and taking

$$\lambda = \frac{\mu_0 i}{4\pi} \quad (\text{A.4})$$

and  $\sin(\theta) = \cos(\alpha)$  ( $\theta = 90^\circ + \alpha$ ) and replacing Eq. (A.3) in Eq. (A.1), the rate of magnetic field is:

$$dB_{cir} = \lambda \frac{dl \cos(\alpha)}{r^2} \quad (\text{A.5})$$

Substituting Eqs. (A.2.a and b) in Eq. (A.6) and considering that  $dl = R d\omega$ , the magnetic field,  $dB$  can be rewritten,

$$dB_{cir} = R\lambda \frac{R - x \cos(\omega)}{(R^2 + x^2 - 2Rx \cos(\omega))^{\frac{3}{2}}} d\omega \quad (\text{A.6})$$

Integrating Eq. (A.5), the magnetic field,  $B(x)$  of a circular coil as shown in Fig. 1a is

$$dB_{cir} = \frac{R\mu_0 i}{4\pi} \int_0^{2\pi} \frac{R - x \cos(\omega)}{(R^2 + x^2 - 2Rx \cos(\omega))^{\frac{3}{2}}} d\omega \quad (\text{A.7})$$

An expression for the magnetic flux can be calculated from Eq. (2)

$$\phi_{cir} = \int_S \left( \frac{R\mu_0 i}{4\pi} \int_0^{2\pi} \frac{R - x \cos(\omega)}{(R^2 + x^2 - 2Rx \cos(\omega))^{\frac{3}{2}}} d\omega \right) dS \quad (\text{A.8})$$

where  $dS = \pi r e^2 - \pi r = \pi(e+1)(e-1) dr$  and

$$dx = r(e-1), \quad x \approx r \frac{e+1}{2}, \quad dS = 2\pi \quad (\text{A.9})$$

therefore inductance is:

$$L_{cir} = \frac{R\mu_0}{4\pi} \int_0^R \int_0^{2\pi} \frac{(R - x \cos(\omega)) x}{(R^2 + x^2 - 2Rx \cos(\omega))^{\frac{3}{2}}} d\omega dx \quad (\text{A.10})$$

### A2. Square-shaped coil

The inductance of a square-shaped coil can be calculated in a similar way to the case of a circular loop. It is only necessary to obtain an expression for the magnetic field,  $\mathbf{B}$  generated by a square loop, Fig 5a shows a square-shaped coil carrying a current  $I$  and where

$$\sin(\theta) = \cos(\beta) \quad (\text{A.11})$$

Hence, the magnetic field  $\mathbf{B}$  of a square-shaped coil for points inside the coil is:

$$dB_{cir} = \frac{\lambda \cos^3(\theta)}{x^2} \quad (\text{A.12})$$

additionally,

$$dl = \sec^2(\beta) d\beta \quad (\text{A.13})$$

replacing Eq. (A.13) in (A.12), we obtained:

$$dB_{sqr} = \frac{x \cos^3(\beta) \sec^2(\beta)}{x^2} = \frac{\lambda \cos(\beta) d\beta}{x} \quad (\text{A.14})$$

(A.14) Integrating Eq. (A.13), an expression for the magnetic field of a square coil can be found:

$$B(x, y)_{sqr} = \int_{-y}^{l-y} \frac{\lambda \cos(\beta) d\beta}{x} = \left| \frac{\lambda}{x} \sin(\beta) \right|_{-y}^{l-y} = \frac{\lambda}{x} \left| \frac{1}{\sqrt{x^2 + l^2}} \right|_{-y}^{l-y} \tag{A.15}$$

Equation (A.15) represents the magnetic field at a point  $P(x,y)$  due to a current  $I$  along a segment of length  $l$ . In this particular geometry, it is necessary to consider all four sides of the square (Fig. 5b). The superposition theorem is used to calculate the total magnetic field at a particular point.

Equation (A.15) can be rewritten to include the four sides:

$$B(x, y)_{sqr} = \frac{\lambda}{x} \left| \frac{1}{\sqrt{x^2 + l^2}} \right|_{-y}^{l-y} + \frac{\lambda}{l-y} \left| \frac{1}{\sqrt{x^2 + l^2}} \right|_{l-x}^{-x} + \frac{\lambda}{l-x} \left| \frac{1}{\sqrt{x^2 + l^2}} \right|_{y-l}^y + \frac{\lambda}{y} \left| \frac{1}{\sqrt{x^2 + l^2}} \right|_{x-l}^x \tag{A.16}$$

(A.16) Developing Eq. (A.16), it can be

$$B(x, y)_{sqr} = \frac{\lambda}{x} \left[ \frac{l-y}{\sqrt{(l-y)^2 + l^2}} + \frac{y}{\sqrt{x^2 + y^2}} \right] + \frac{\lambda}{l-y} \left[ \frac{l-x}{\sqrt{(l-x)^2 + (l-y)^2}} + \frac{x}{\sqrt{x^2 + (l-y)^2}} \right] + \frac{\lambda}{l-x} \left[ \frac{y}{\sqrt{y^2 + (l-x)^2}} + \frac{l-y}{\sqrt{(l-x)^2 + (l-y)^2}} \right] + \frac{\lambda}{y} \left[ \frac{x}{\sqrt{x^2 + y^2}} + \frac{l-x}{\sqrt{y^2 + (l-x)^2}} \right] \tag{A.17}$$

Prior to obtaining an expression for the inductance of square-shaped coil, a formula for the magnetic flux should be found, then from Eq. (2) the magnetic flux is:

$$B(x, y)_{sqr} = \int_S \left( \frac{\lambda}{x} \left[ \frac{l-y}{\sqrt{(l-y)^2 + l^2}} + \frac{y}{\sqrt{x^2 + y^2}} \right] + \frac{\lambda}{l-y} \left[ \frac{l-x}{\sqrt{(l-x)^2 + (l-y)^2}} + \frac{x}{\sqrt{x^2 + (l-y)^2}} \right] \right) \bullet dS + \int_S \left( \frac{\lambda}{l-x} \left[ \frac{y}{\sqrt{y^2 + (l-x)^2}} + \frac{l-y}{\sqrt{(l-x)^2 + (l-y)^2}} \right] + \frac{\lambda}{y} \left[ \frac{x}{\sqrt{x^2 + y^2}} + \frac{l-x}{\sqrt{y^2 + (l-x)^2}} \right] \right) \bullet dS \tag{A.18}$$

To solve Eq. (B.8) it is necessary to obtain the integral limits for each side of the square in Fig. 5b and 5c, so that it becomes,

$$\phi_{sqr} = \frac{\mu_0 i}{4\pi} \int_0^x \int_0^y \left( \frac{\lambda}{x} \left[ \frac{l-y}{\sqrt{(l-y)^2 + l^2}} + \frac{y}{\sqrt{x^2 + y^2}} \right] + \frac{\lambda}{l-y} \left[ \frac{l-x}{\sqrt{(l-x)^2 + (l-y)^2}} + \frac{x}{\sqrt{x^2 + (l-y)^2}} \right] \right) dydx + \frac{\mu_0 i}{4\pi} \int_0^x \int_0^y \left( \frac{\lambda}{l-x} \left[ \frac{y}{\sqrt{y^2 + (l-x)^2}} + \frac{l-y}{\sqrt{(l-x)^2 + (l-y)^2}} \right] + \frac{\lambda}{y} \left[ \frac{x}{\sqrt{x^2 + y^2}} + \frac{l-x}{\sqrt{y^2 + (l-x)^2}} \right] \right) dydx \tag{A.19}$$

Finally, the inductance formula is

$$L_{sqr} = \frac{\mu_0}{4\pi} \int_0^x \int_0^y \left( \frac{\lambda}{x} \left[ \frac{l-y}{\sqrt{(l-y)^2 + l^2}} + \frac{y}{\sqrt{x^2 + y^2}} \right] + \frac{\lambda}{l-y} \left[ \frac{l-x}{\sqrt{(l-x)^2 + (l-y)^2}} + \frac{x}{\sqrt{x^2 + (l-y)^2}} \right] \right) dydx + \frac{\mu_0}{4\pi} \int_0^x \int_0^y \left( \frac{\lambda}{l-x} \left[ \frac{y}{\sqrt{y^2 + (l-x)^2}} + \frac{l-y}{\sqrt{(l-x)^2 + (l-y)^2}} \right] + \frac{\lambda}{y} \left[ \frac{x}{\sqrt{x^2 + y^2}} + \frac{l-x}{\sqrt{y^2 + (l-x)^2}} \right] \right) dydx \tag{A.20}$$

- \*. Corresponding author: Alfredo O. Rodríguez, Centro de Investigación en Imagenología e Instrumentación Médica, Universidad Autónoma Metropolitana Iztapalapa, Av. San Rafael Atlixco 186, México, D. F., 09340. México. Telephone No.: (5255) 85024569, Fax No.: (5255) 804-4631, e-mail: arog@xanum.uam.mx.
- \*\* Present Address: Institute of Imaging Science, Vanderbilt University, Nashville TN 37232-2675, USA.
1. J.J.H. Ackerman, T.H. Grove, G.G. Wong, D.G. Gadian, and G.K. Radda, *Nature* **283** (1980) 167.
  2. A.O. Rodriguez, *Rev. Mex. Fís.* **50** (2004) 272.
  3. The International Society for Magnetic Resonance in Medicine, *RF Bootcamp: Essential of RF coil design, construction and interface*. (Knowledge Access Publishing, Connecticut, 1999), CD ROM.
  4. P.B. Roemer, W.A. Edelstein, C.E. Hayes, S.P. Souza, and O.M. Muller, *Magn. Reson. Med.* **16** (1990) 192.
  5. K.P. Pruessmann, M. Weiger, M.B. Scheidegger, and P. Boesiger, *Mag. Reson. Med.* **42** (1999) 952.
  6. D.K. Sodickson and W.J. Manning, *Mag. Reson. Med.* **38** (1998) 591.
  7. S. Hidalgo *et al.*, *Proc. 9th Ann. Meet. of ISMRM*, 112 (2001).
  8. M.A. López Terrones, *Antena superficial tipo magnetron plano de 8 cavidades para Espectroscopía por Resonancia Magnética a 1.5 T, 3 T y 7 T*, Master's Thesis, Biomedical Engineering Graduate Programme, Universidad Autonoma Metropolitana Iztapalapa, 2004, Mexico.
  9. S.E. Solís Nájera, *Antena superficial PERES con envolvente circular para IRM*, Master's Thesis, Biomedical Engineering Graduate Programme, Universidad Autonoma Metropolitana Iztapalapa, 2004, Mexico.
  10. R. Hernandez, A.O. Rodriguez, J. Sanchez Cortazar, P. Salgado, and F. A. Barrios, *Folded Crossed-Ellipse Coil for Hand MRI. Proc. 25th Ann. Int. Con. IEEE Eng. Med. Biol.* Cancun, Mexico, (2003) 497.
  11. O. Marrufo, *Jornadas del Posgrado de Ciencias Básicas*, UAM Iztapalapa, (2004).
  12. D.I. Hoult, *Prog. NMR Spect.*, **12** (1978) 41.
  13. D.I. Hoult and R.E. Richardson, *J. Magn. Reson.* **24** (1976) 71.
  14. J. Wang, A. Reykowski, and J. Dickas, *IEEE Trans. Biom. Eng.* **42** (1995) 908.
  15. J. Jin, *Electromagnetic Analysis and Design* (CRC Press, Boca Raton, 1999) 137.
  16. J.D. Jackson, *Classical Electrodynamics* (John Wiley, New York, 1999), 3rd Edition, 215-223.
  17. M. Bueno and A.K.T. Assis, *Can. J. Phys.* **75** (1997) 357.
  18. F.E. Terman, *Radio engineer's handbook* (MacGraw-Hill, New York, 1943).
  19. A. Ouldkhal, B. Bandelier, S. Kan, and F. Rious-Damidau, *IEEE on Mag.* **31** (1995) 1590.
  20. M. Gyimesi and D. Ostergaard, *IEEE on Mag.* **35** (1999) 1119.
  21. C.A. Balanis, *Antenna theory: analysis and design* (John Wiley, New York, 1997), 2nd Edition, 468.
  22. R.P. Feynman, R.B. Leighton, and M. Sands, *The Feynman lectures on physics: The electromagnetic field* (Addison-Wesley, Reading, 1964), Vol. II, 1.
  23. E.M. Purcell, *Electricity and magnetism*, (MacGraw-Hill, New York, 1965) Berkely Physics Course, Vol. II, 250.
  24. E.C. Jordan, *Electromagnetic waves and radiating systems* (Prentice Hall, Englewood Cliffs, 1958) 211.
  25. J.R. Reitz and F.J. Milford, *Foundations of electromagnetic theory* (Addison-Wesley, Reading, 1960) 170.
  26. W.T. Sobol, *Rev. Magn. Reson. Med.* **1** (1986) 181.
  27. C.N. Chen and D.I. Hoult, *Biomedical Magnetic Resonance Technology* (Adam Hilger, Institute of Physics Publishing, Britain, 1989). pp. 117-226.
  28. C.E. Hayes, W.A. Edelstein, and J.F. Schenck, *Radio Frequency Coils*, in S.R. Thomas and R.L. Dixon, *NMR in Medicine: The Instrumentation and Clinical Applications* (American Institute of Physics Publishing, New York, 1986) 142.
  29. E. Krestel, *Imaging systems for medical diagnostics; fundamentals and technical solutions; X-ray diagnostics, computed tomography, nuclear medical medicine diagnostics, magnetic resonance imaging, sonography, biomagnetic diagnostics* (Siemens-Aktienges, Berlin, 1090) 479.
  30. R. Amador Baheza, *Desarrollo de antenas superficiales de radiofrecuencia para imagenología por resonancia magnética*, Master's Thesis, Biomedical Engineering Graduate Programme, Universidad Autonoma Metropolitana Iztapalapa, (2001) México.